Effects of different structural parameters and the medium environment on plasmonic lattice resonance formed by Ag nanospheres on SiO_2 nanopillar arrays

Xiaodan Huang (黄小丹)[1,2,*], Chaogang Lou (娄朝刚)[2,], Hao Zhang (张 浩)[2,3], and Hua Yang (杨 桦)[2]**

[1]*Professional Basic Department, Changzhou Vocational Institute of Mechatronic Technology, Changzhou 213164, China*

[2]*Joint International Research Laboratory of Information Display and Visualization, School of Electronic Science and Engineering, Southeast University, Nanjing 210096, China*

[3]*Public Resource Trading Center, Municipal Administrative Services Management Bureau, Lianyungang 222006, China*

**Corresponding author: hxd@seu.edu.cn; **corresponding author: lcg@seu.edu.cn*

Received September 30, 2019; accepted December 11, 2019; posted online February 18, 2020

The effects of the diameter of SiO_2 nanopillars, the diameter of Ag nanospheres, the arrays' period, and the medium environment on the plasmonic lattice resonance (PLR) formed by Ag nanospheres on SiO_2 nanopillar arrays are systematically investigated. Larger diameters of SiO_2 nanopillars with other parameters kept constant will widen the PLR peak, redshift the PLR wavelength, and weaken the PLR intensity. Larger diameters of Ag nanospheres with other parameters kept constant will widen the PLR peak, redshift the PLR wavelength, and strengthen the PLR intensity. Larger array periods or larger refractive index of medium environment corresponds to larger PLR wavelengths.

Keywords: plasmonics; diffraction theory; resonance; multilayer design.
doi: 10.3788/COL202018.033601.

Periodic metallic nanoparticle arrays can form plasmonic lattice resonance (PLR) with narrower spectral linewidths and higher field enhancement than those of localized surface plasmonic resonance of single isolated metallic nanoparticles[1,2]. The unique nature can be explained by the coupling between the diffraction of light and the localized surface plasmon resonances of the metallic nanoparticles[3–9]. Some researchers have shown that the remarkable properties of PLR offer new opportunities for many applications, such as optical instruments[10,11], spectral signals[12–14], and sensors[15–18]. However, in practical applications, metallic nanoparticle arrays often need a substrate to support them. This suppresses the formation of PLR due to the mismatch of the refractive index between the superstrate and the substrate.

In order to promote the application of PLR, many methods have been proposed. Some of them covered the metallic nanoparticles with solid[19–21] or liquid[22] materials with similar refractive index to the substrate material. But this method may not be suitable for the potential applications of some special devices (e.g., some special sensors need gas as a superstrate). Others have reported that, when the metallic nanoparticles are big enough to show a significant scattering cross section or polarizability, PLR can be formed even if the metallic nanoparticle arrays are in inhomogeneous surroundings[23,24]. But the requirement of the large metallic nanoparticle makes it impossible to fabricate the arrays with a small period and form PLR in shorter wavelength ranges. This may limit the application of PLR in some luminescence materials (because PLR has been shown to enhance the light emission from plastic scintillators at short wavelengths)[13].

Recently, we found that the structure of the metallic nanoparticles on the dielectric nanopillar arrays can form PLR[25,26]. This is due to the fact that the dielectric nanopillar arrays provide a more uniform dielectric environment to the metallic nanoparticle arrays. However, the structural parameters and the medium environment on the PLR formed by the metallic nanoparticles on the dielectric nanopillar arrays have been unclear so far, and the specific mechanism of the PLR needs to be clarified further.

In this work, the effects of different structural parameters (including the diameter of SiO_2 nanopillars, the diameter of Ag nanospheres, and the period of the arrays) and the medium environment on the PLR formed by Ag nanospheres on SiO_2 nanopillar arrays that sit on a quartz substrate are systematically investigated. The origin of the PLR is clarified further. This work provides a theoretical basis for the design of excellent PLR structures.

Figure 1 shows the simulated structure. SiO_2 nanopillars have the height of 300 nm. The diameter (D_{SiO2}) of SiO_2 nanopillars varies from 60 nm to 360 nm. The diameter (D_{Ag}) of Ag nanospheres varies from 80 nm to 160 nm. The periods (P) of the arrays in the x and y directions remain the same and vary from 400 nm to 600 nm. The refractive index (n) of the medium environment varies from 1 to 1.5 with the step of 0.1. An incident light propagates along the z direction. The refractive indexes of Ag

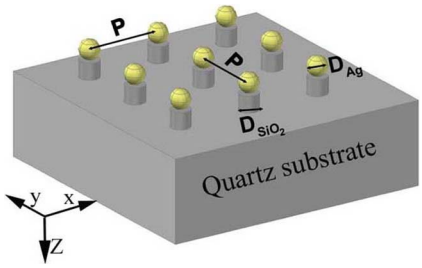

Fig. 1. Schematic of the periodic arrays with Ag nanospheres on SiO_2 nanopillars that sit on a quartz substrate.

are obtained from Palik[27]. The refractive index of the quartz and SiO_2 is set as a constant value of 1.5[27]. The simulation is carried out by using the finite element method. In the simulation, perfectly matched layers are introduced at the top and bottom surfaces of the modeling unit, and the side surfaces in the x and y directions are set as periodic boundary conditions. The transmittance is defined as the ratio of the power of light entering the substrate to the incident light power[25].

Figure 2(a) shows the transmission curves of Ag nanospheres on SiO_2 nanopillar arrays with different diameters. It can be seen that, in each curve, the transmittance changes from the maximum (e.g., at 450 nm for $D_{SiO2} = 120$ nm) to the minimum (e.g., at 478 nm for $D_{SiO2} = 120$ nm) in a narrow wavelength band[25]. The minimum transmittance originates from the PLR, which corresponds to the maximum extinction cross section [as shown in Fig. 2(b)] and the maximum electric field intensity [as shown in Fig. 2(c)] of Ag nanosphere arrays. However, when the diameter of SiO_2 nanopillars increases (with other parameters kept constant), the transmittance at dip's position increases, the dips in the transmittance curve become broader, and the wavelength position of the dips shifts to the red. When the diameter of SiO_2 nanopillars reaches 360 nm, the dip in the transmittance curve is very weak and almost disappears. These results indicate that the larger diameter of SiO_2 nanopillars (with other parameters kept constant) will widen the PLR peak, redshift the PLR wavelength, and reduce the PLR intensity.

The differences in the transmittance of Ag nanospheres on SiO_2 nanopillar arrays with different diameters can be explained by the coupling between the diffraction of the periodic arrays and the localized surface plasmonic resonance of Ag nanospheres.

For the structure of Ag nanospheres on SiO_2 nanopillar arrays with the diameter of 120 nm, the coverage of SiO_2 nanopillar arrays is only 5.6% and the equivalent refractive index of SiO_2 nanopillar arrays is close to that of air, and so, SiO_2 nanopillar arrays can provide Ag nanospheres with an approximately homogeneous surrounding. When the incident wavelength is equal to the period (450 nm) of the arrays, the first-order diffracted wave in the air is the strongest (because it propagates in the direction that parallels with the substrate's surface)[25,28,29]. They dissipate the largest energy from Ag nanospheres

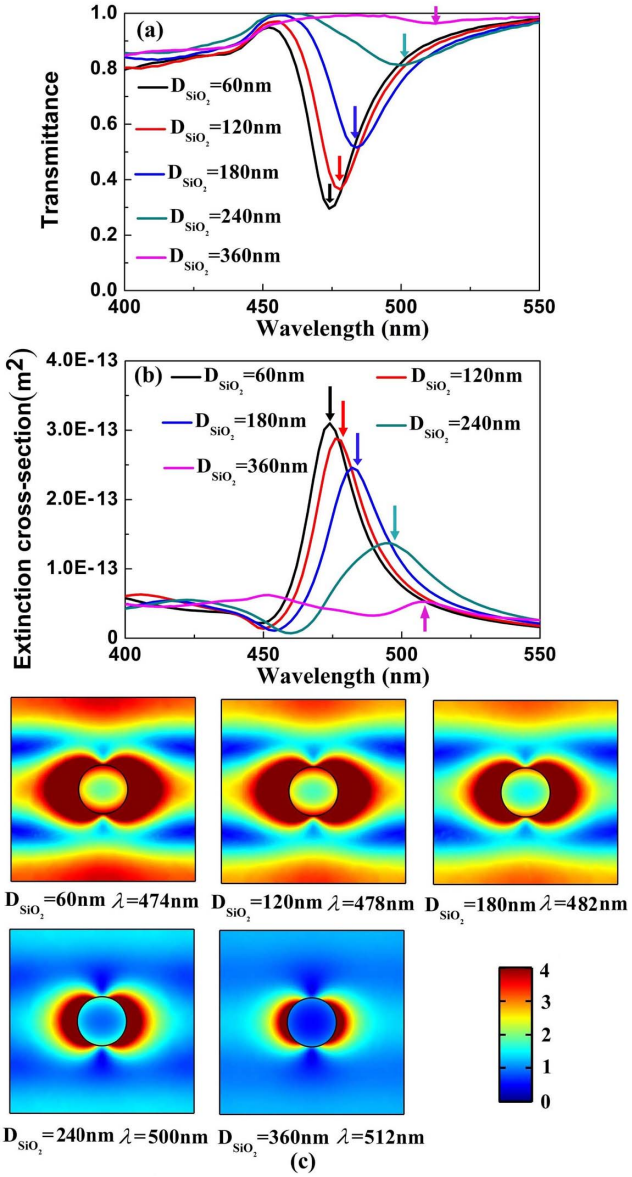

Fig. 2. (a) Simulated transmittance and (b) extinction cross section of Ag nanospheres on SiO_2 nanopillar arrays with different diameters of 60, 120, 180, 240, and 360 nm, respectively. (c) The electric field intensity on the $x-y$ plane through the center of Ag nanospheres on SiO_2 nanopillar arrays with different diameters with the same color bar. ($P = 450$ nm, $D_{Ag} = 120$ nm, $n = 1$.)

and weaken their resonance[25,28,29]. As a result, at the wavelength of 450 nm, the extinction cross section of Ag nanospheres reaches the minimum [as shown in Fig. 2(b)] and the transmittance reaches the maximum, as shown in Fig. 2(a).

However, when the wavelength is beyond 450 nm, the first-order diffracted waves in the air disappear rapidly and the dissipated energy also decreases quickly. This strengthens Ag nanospheres' resonance and increases the extinction cross section of Ag nanospheres quickly. On the other hand, the resonance of Ag nanospheres in the arrays is weakened [because the incident wavelength moves away from the localized surface plasmonic

resonance wavelength (440 nm) of single isolated Ag nanospheres, as shown in Fig. 4], and so Ag nanospheres' extinction cross section decreases. The competition between these two mechanisms results in the maximum extinction cross section of Ag nanospheres and the minimum transmittance of the structure around 478 nm.

When the diameter of SiO_2 nanopillars increases (with other parameters kept constant), the coverage of SiO_2 nanopillar arrays increases and the equivalent refractive index of SiO_2 nanopillar arrays also increases. This increases the asymmetry of the diffraction in the air and in the substrate. At the PLR wavelengths, the first-order diffracted waves in the air disappear, but the diffracted waves in the substrate do not vanish and become stronger as the diameter of SiO_2 nanopillars increases, and so more energy is dissipated from Ag nanospheres and their extinction cross section decreases. Thus, the transmittance at the dip's position increases as the diameter of SiO_2 nanopillars increases. Correspondingly, when the diameter of SiO_2 nanopillars reaches 360 nm, the dip in the transmittance curve is very weak and almost disappears, and the PLR intensity is weakened greatly.

Figure 2(b) shows the extinction cross section curve of Ag nanospheres on SiO_2 nanopillar arrays with different diameters. It is clear that, the maximum extinction cross section in each curve corresponds to the minimum transmittance in corresponding curve [in Fig. 2(a)]. Meanwhile, the extinction cross section peak becomes broader and gradually shifts to the red as the diameter of SiO_2 nanopillars increases (when the other parameters kept constant).

Figure 2(c) shows the electric field intensity around Ag nanospheres on SiO_2 nanopillar arrays with different diameters. It can be seen that, at PLR wavelengths, the electric field intensity is weakened with the increasing diameter of SiO_2 nanopillars (when the other parameters kept constant). This agrees with the explanation about the transmittance and the extinction cross section.

Figures 3(a) and 3(b) show the spectra of transmittance of Ag nanospheres with different diameters on SiO_2 nanopillar arrays. It can be seen that, with the increasing diameter of Ag nanospheres (when the other parameters kept constant), the transmittance spectrum of the structure gradually shifts to the red, the transmittance dip becomes broader, and the transmittance at the dip's position lowers further. Figure 3(c) shows the minimum transmittance (corresponding to PLR) wavelength plotted versus Ag nanospheres' diameter. It can be seen that, when Ag nanospheres' diameter increases from 80 nm to 160 nm, the minimum transmittance wavelength shifts from 454 nm to 505 nm. These results indicate that larger diameters of Ag nanospheres (with other parameters kept constant) will cause the redshift of the PLR wavelength, widen the PLR peak, and enhance the PLR intensity.

The phenomena can be explained by the localized surface plasmonic resonance of Ag nanospheres. When the diameter of Ag nanospheres increases (with other parameters kept constant), the localized surface plasmonic

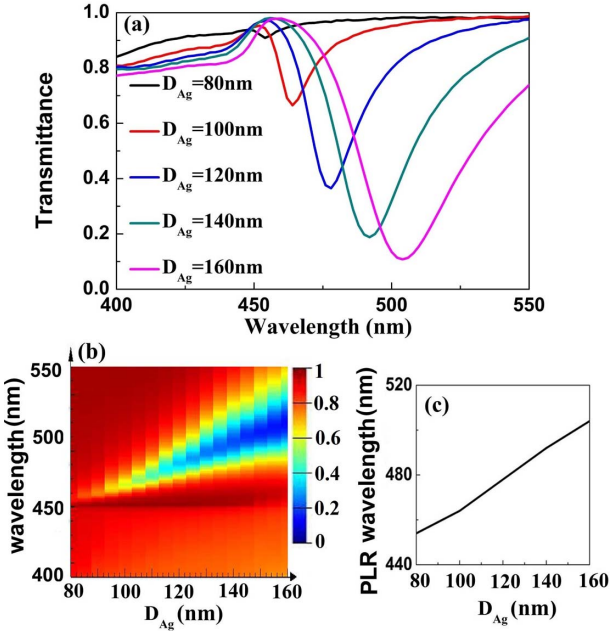

Fig. 3. (a) The simulated transmittance of Ag nanospheres on SiO_2 nanopillar arrays with different Ag nanospheres' diameters of 80, 100, 120, 140, and 160 nm, respectively. (b) The transmittance of Ag nanospheres on SiO_2 nanopillar arrays as a function of Ag nanospheres' diameter (D_{Ag}) and the wavelength, which is plotted in 3D format. (c) The PLR (corresponding to the minimal transmittance) wavelength plotted versus Ag nanospheres' diameter. ($P = 450$ nm, $D_{SiO2} = 120$ nm, $n = 1$.)

resonance of single isolated Ag nanospheres becomes stronger, the resonance peak becomes broader, and the resonance wavelength shifts to the red. Figure 4 shows the simulated extinction cross sections of a single Ag nanosphere with different diameters. Because the PLR originates from the coupling between the diffraction of the periodic arrays and the localized surface plasmonic resonance of Ag nanospheres, with the increasing diameter of Ag nanospheres (with other parameters kept constant), the stronger localized surface plasmonic resonance, the wider resonance peak, and the redshift of the localized

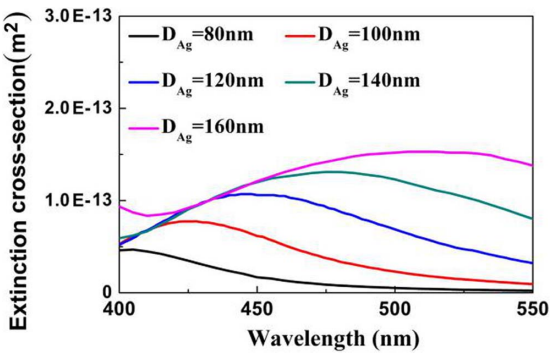

Fig. 4. Simulated extinction cross section of a single Ag nanosphere with different diameters of 80, 100, 120, 140, and 160 nm on a SiO_2 nanopillar that sits on a quartz substrate, respectively. ($D_{SiO2} = 120$ nm, $n = 1$.)

surface plasmonic resonance wavelength result in stronger PLR intensity, broader PLR peak, and the redshift of the PLR wavelength, respectively.

Figures 5(a) and 5(b) show the spectra of transmission of Ag nanospheres on SiO_2 nanopillar arrays at different periods. It can be seen that, with the increasing period of the arrays (with other parameters kept constant), the transmittance curve (including the PLR wavelength) gradually shifts to the red and the transmittance at the PLR wavelength increases. Figure 5(c) shows the PLR wavelength plotted versus the period of the array. It can be seen that, when the arrays' period increases from 400 nm to 600 nm, the PLR wavelength shifts from 453 nm to 600 nm.

The phenomena in Fig. 5 can be explained by the diffraction theory. When the period of the arrays increases, the wavelength position of the surface diffraction waves (which propagate in the direction that parallels with the substrate's surface) shifts to the red (because the wavelength position of the surface diffraction waves is proportional to the period of the arrays and the refractive index of the medium environment[19,20]), and so the wavelength position of the PLR (corresponding to the transmittance dip) also shifts to the red.

In addition, with the increasing period of the arrays, because the wavelength position of the first-order diffraction waves in the air moves away from the localized surface plasmonic resonance wavelength (440 nm) of Ag nanospheres, the coupling between the diffraction of the periodic arrays and the localized surface plasmonic resonance of Ag nanospheres becomes weak. As a result, with the increasing period of the arrays (when other parameters are kept constant), the PLR intensity is weakened and the transmittance at the dip's position is increased [as shown in Figs. 5(a) and 5(b)].

From the above discussions, it can be known that PLR is very sensitive to the changes of different structural parameters. The intensity, peak, and wavelength position of the PLR can be controlled and optimized by adjusting the diameter of SiO_2 nanopillars, the diameter of Ag nanospheres, and the period of the arrays.

Figures 6(a) and 6(b) show the spectra of transmittance of Ag nanospheres on SiO_2 nanopillar arrays in different media environments. It can be seen that the dip (corresponding to the PLR peak) in each transmission curve can be observed. When the refractive index of the medium environment increases (with the structural parameters kept constant), because the wavelength position of the surface diffraction waves gradually shifts to the red due to the diffraction theory[28,29], this makes the PLR wavelength also gradually shift to the red.

Additionally, it can be observed from Fig. 6(a) that the minimum half-width of the dip (for $n = 1.5$) in the transmittance curve is about 15 nm, and the half-width is not sensitive to the refractive index of the medium environment. The consequence of this observation is important because it indicates that this structure can provide good stability and universal applicability.

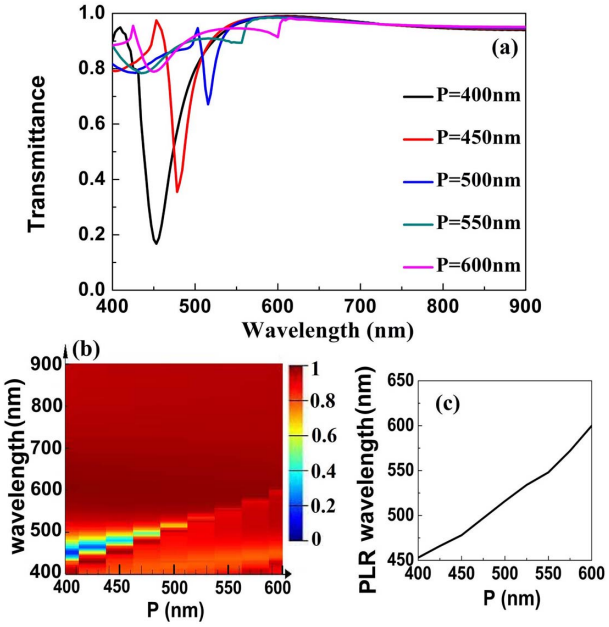

Fig. 5. (a) The simulated transmittance of Ag nanospheres on SiO_2 nanopillar arrays at different periods of 400, 450, 500, 550, and 600 nm. (b) The transmittance of Ag nanospheres on SiO_2 nanopillar arrays as a function of the arrays' period (P) and the wavelength, which is plotted in 3D format. (c) The PLR wavelength plotted versus the arrays' period. ($D_{Ag} = D_{SiO2} = 120$ nm, $n = 1$.)

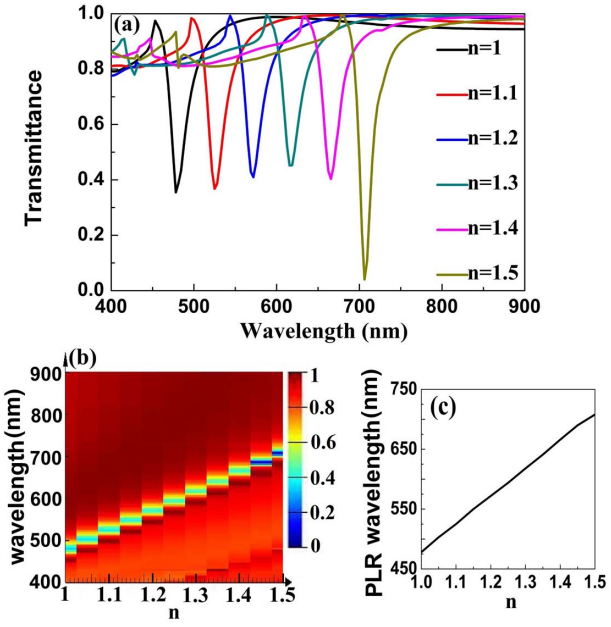

Fig. 6. (a) The simulated transmittance of Ag nanospheres on SiO_2 nanopillar arrays in different media environments. (b) The transmittance of Ag nanospheres on SiO_2 nanopillar arrays as a function of the refractive index (n) of the media environment and the wavelength, which is plotted in 3D format. (c) The PLR wavelength plotted versus the refractive index of the media environment. ($D_{Ag} = D_{SiO2} = 120$ nm, $P = 450$ nm.)

Since the wavelength position of the PLR depends on the refractive index of the surrounding medium environment, the change of the refractive index of the medium environment can be detected by monitoring the transmittance near the PLR wavelength. The PLR wavelength versus the refractive index (n) of the medium environment is plotted in Fig. 6(c). It can be seen that, when the refractive index of the medium environment increases from 1 to 1.5, the PLR wavelength almost shifts linearly from 478 nm to 708 nm. The calculated sensitivity [which is defined as the PLR wavelength shift per refractive index unit (RIU)] of the structure is 460 nm/RIU, which is higher than that (365 nm/RIU) of the previously reported hexagonal arrays[15]. The high sensitivity together with a small half-width of this structure may provide potential advantages in the application of sensors.

In conclusion, the effects of different structural parameters (including the diameter of SiO_2 nanopillars, the diameter of Ag nanospheres, and the period of the arrays) and the medium environment on the plasmonic lattice resonance formed by Ag nanospheres on SiO_2 nanopillar arrays are systematically investigated. The simulated results show that larger diameters of SiO_2 nanopillars (with other parameters kept constant) will widen the PLR peak, cause the redshift of the PLR wavelength, and reduce the PLR intensity. Increasing the diameter of Ag nanospheres (with other parameters kept constant) will enhance the PLR intensity, shift the PLR wavelength to the red, and widen the PLR peak. Furthermore, it is found in the simulation that, with the increasing period of the arrays or with the increasing refractive index of the medium environment, the PLR wavelength is redshifted. This is because the PLR wavelength is proportional to both the period of the arrays and the refractive index of the medium environment. These results are relatively instructive and meaningful for the design of excellent PLR structures.

This work was supported by the Primary Research & Development Plan of Jiangsu Province (No. BE2016175) and the Chinese Postdoctoral Science Foundation (No. 2017M621581).

References

1. A. V. Kabashin, A. G. Nikitin, and H. Dallaporta, Opt. Express **20**, 27941 (2012).
2. Y. Chu, E. Schonbrun, T. Yang, and K. B. Crozier, Appl. Phys. Lett. **93**, 357 (2008).
3. A. Hajebifard and P. Berini, Opt. Express **25**, 18566 (2017).
4. L. Michaeli, S. Keren-Zur, O. Avayu, H. Suchowski, and T. Ellenbogen, Phys. Rev. Lett. **118**, 243904 (2017).
5. K. Sakai, K. Nomura, T. Yamamoto, T. Omura, and K. Sasaki, Sci. Rep. **6**, 34967 (2016).
6. C. J. Tang, P. Zhan, Z. S. Cao, J. Pan, Z. Chen, and Z. L. Wang, Phys. Rev. B **83**, 53 (2011).
7. B. Auguié, X. M. Bendaña, W. L. Barnes, and F. Jarcía de Abajo, Phys. Rev. B **82**, 557 (2010).
8. V. G. Kravets, F. Schedin, and A. N. Grigorenko, Phys. Rev. Lett. **101**, 087403 (2008).
9. D. Dejarnette, J. Norman, and D. K. Roper, Photon. Res. **2**, 15 (2014).
10. M. J. Huttunen, P. Rasekh, R. W. Boyd, and K. Dolgaleva, Phys. Rev. A **97**, 053817 (2018).
11. T. K. Hakala, H. T. Rekola, A. I. Väkeväinen, J. P. Martikainen, M. Nečada, A. J. Moilanen, and P. Törmä, Nat. Commun. **8**, 13687 (2017).
12. V. Giannini, G. Vecchi, and J. Gómez Rivas, Phys. Rev. Lett. **105**, 266801 (2010).
13. B. Liu, Z. Zhu, Q. Wu, C. Cheng, M. Gu, J. Xu, H. Chen, J. Liu, L. Chen, and X. Ouyang, Appl. Phys. Lett. **110**, 31 (2017).
14. Z. Qi, J. Yao, L. Zhao, Y. Cui, and C. Lu, Photon. Res. **3**, 313 (2015).
15. A. I. Kuznetsov, A. B. Evlyukhin, M. R. Gonçalves, C. Reinhardt, A. Koroleva, M. L. Arnedillo, R. Kiyan, O. Marti, and B. N. Chichkov, ACS Nano **5**, 4843 (2011).
16. P. Offermans, M. C. Schaafsma, S. R. K. Rodriguez, Y. Zhang, M. Crego-calama, S. H. Brongersma, and J. G. Rivas, ACS Nano **5**, 5151 (2011).
17. J. Li, C. Chen, L. Lagae, and P. V. Dorpe, J. Phys. Chem. C **119**, 29116 (2015).
18. J. Ma, D. Liu, J. Wang, and Z. Hu, Chin. Opt. Lett. **16**, 032301 (2018).
19. S. M. Sadeghi, R. R. Gutha, and W. J. Wing, Opt. Lett. **41**, 3367 (2016).
20. S. M. Sadeghi, W. J. Wing, and Q. Campbell, J. Appl. Phys. **119**, 021019 (2016).
21. W. J. Wing, S. M. Sadeghi, and R. R. Gutha, J. Appl. Phys. **120**, 234301 (2016).
22. B. Auguié and W. L. Barnes, Phys. Rev. Lett. **101**, 143902 (2008).
23. A. G. Nikitin, T. Nguyen, and H. Dallaporta, Appl. Phys. Lett. **102**, 221116 (2013).
24. A. Vitrey, L. Aigouy, P. Prieto, J. M. García-Martín, and M. U. González, Nano Lett. **14**, 2079 (2014).
25. X. Huang, C. Lou, H. Zhang, and D. Pribat, Plasmonics **14**, 241 (2019).
26. X. Huang, C. Lou, and H. Zhang, J. Phys. D **51**, 465101 (2018).
27. E. D. Palik, *Handbook of Optical Constants of Solids* (Academic Press, 1985).
28. M. Meier, A. Wokaun, and P. F. Liao, J. Opt. Soc. Am. B **2**, 931 (1985).
29. K. T. Carron, W. Fluhr, M. Meier, and A. Wokaun, J. Opt. Soc. Am. B **3**, 430 (1986).